

# Pressure-induced superconductivity in flat-band Kagome compounds $\text{Pd}_3\text{P}_2(\text{S}_{1-x}\text{Se}_x)_8$

Shuo Li,<sup>1,2,\*</sup> Shuo Han,<sup>2,\*</sup> Shaohua Yan,<sup>2,\*</sup> Yi Cui,<sup>2</sup> Le Wang,<sup>2</sup> Shanmin Wang,<sup>3</sup> Shanshan Chen,<sup>2</sup> Hechang Lei,<sup>2,†</sup> Feng Yuan,<sup>4,‡</sup> J. S. Zhang,<sup>1,§</sup> and Weiqiang Yu<sup>2,¶</sup>

<sup>1</sup>*Mathematics and Physics Department, North China Electric Power University, Beijing 102206, China*

<sup>2</sup>*Department of Physics and Beijing Key Laboratory of Opto-electronic Functional*

*Materials & Micro-nano Devices, Renmin University of China, Beijing, 100872, China*

<sup>3</sup>*Department of Physics, Southern University of Science & Technology, Shenzhen, Guangdong, 518055, China*

<sup>4</sup>*College of Physics, Qingdao University, Qingdao 266071, China*

We performed high-pressure transport studies on the flat-band Kagome compounds,  $\text{Pd}_3\text{P}_2(\text{S}_{1-x}\text{Se}_x)_8$  ( $x = 0, 0.25$ ), with a diamond anvil cell. For both compounds, the resistivity exhibits an insulating behavior with pressure up to 17 GPa. With pressure above 20 GPa, a metallic behavior is observed at high temperatures in  $\text{Pd}_3\text{P}_2\text{S}_8$ , and superconductivity emerges at low temperatures. The onset temperature of superconducting transition  $T_C$  rises monotonically from 2 K to 5 K and does not saturate with pressure up to 43 GPa. For the Se-doped compound  $\text{Pd}_3\text{P}_2(\text{S}_{0.75}\text{Se}_{0.25})_8$ , the  $T_C$  is about 1.5 K higher than that of the undoped one over the whole pressure range, and reaches 6.5 K at 43 GPa. The upper critical field with field applied along the  $c$  axis at typical pressures is about 50% of the Pauli limit, suggests a 3D superconductivity. The Hall coefficient is low and exhibits a peaked behavior at about 40 K, which suggests a multi-band electronic structure.

Kagome lattice systems have been proposed to host rich physics, such as quantum spin liquid and unconventional superconductivity in systems with strong electron correlations<sup>1–5</sup>. Recently, the electronic flat band<sup>6–15</sup> and Dirac cones<sup>9–11,16–22</sup> were also observed and caused intense research interests in several metallic kagome materials, where the electron correlations appear to be weak. In the Kagome lattice, the flat band arises from phase destruction of electron wave functions in the corner shared triangles, so that one electron band is localized in the hexagons<sup>23,24</sup>. Theoretically, the high electronic density of states in the flat band is expected to enhance the correlation effect if the flat band is close to the Fermi surface, which may give rise to unusual phenomena such as high  $T_C$  superconductivity<sup>25,26</sup>, fractional quantum Hall effect<sup>27</sup> and ferromagnetism<sup>28,29</sup>.

Unfortunately, the electron correlations in the flat-band Kagome materials seems to be too weak to offer any novel phase so far<sup>6–15</sup>. In parallel, signatures of flat bands and the related novel phases have been discovered experimentally in twisted bilayer graphene<sup>30,31</sup>, silicene<sup>32</sup> and dichalcogenides<sup>33</sup>. An alternative way to look for novel phases is to tune the materials by doping or pressure<sup>34,35</sup>, so that the electrons can be partly delocalized and bring in the electron correlation effect. In this regard, candidate Kagome materials having flat band close to Fermi surface, such as  $\text{CoSn}$ <sup>9,10,36</sup> and  $\text{Pd}_3\text{P}_2\text{S}_8$ <sup>14,15</sup>, are favored for further study by doping or pressure tuning.

Here we report our high-pressure transport studies on a van-der-Waals (vdW) Kagome compound  $\text{Pd}_3\text{P}_2\text{S}_8$  and its Se-doped compound  $\text{Pd}_3\text{P}_2(\text{S}_{0.75}\text{Se}_{0.25})_8$ , both of which are highly insulating at the ambient pressure<sup>14,15</sup>. Pd atoms in  $\text{Pd}_3\text{P}_2\text{S}_8$  constitute the Kagome plane, as shown in Fig. 1. LDA calculations on  $\text{Pd}_3\text{P}_2\text{S}_8$  reveals that a flat band, mainly formed by the  $d_{z^2}$  orbital of  $\text{Pd}^{2+}$ , is located at about 0.2 eV below the Fermi surface<sup>15</sup>. Se doping enhances the interlayer coupling and reduces the gap of the flat band<sup>15</sup>.

Our high-pressure transport studies show that for both compounds, the conductivity at 300 K is enhanced under pressure. At about 17 GPa, an insulating behavior is still seen. How-

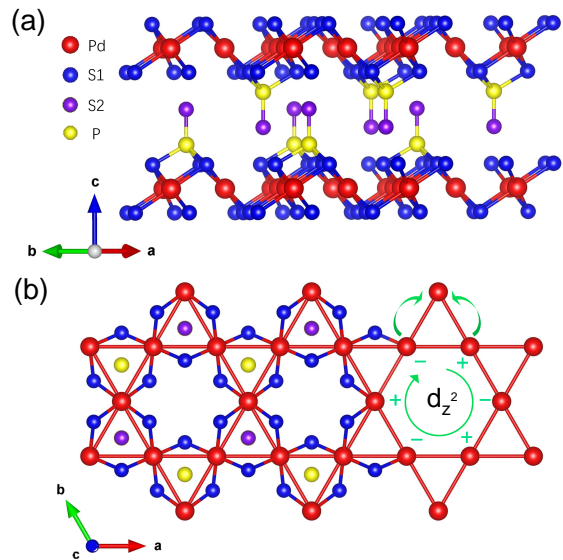


FIG. 1. (a) Planar view of the crystal structure of  $\text{Pd}_3\text{P}_2\text{S}_8$ . (b) Top view of one kagome layer. Phase destruction of the electron hopping is illustrated in a triangle, and electron localization is present in the hexagon.  $d_{z^2}$  labels the primary orbital that forms the flat band.

ever, their conductivity exhibits a power-law temperature dependence in two decades of temperature below 300 K, which suggests strong electron localization caused by disorder<sup>37</sup>. With further increase of pressure above 20 GPa, a metallic behavior is induced at high temperatures. Superconductivity emerges at low temperatures in the metallic phase. The upper critical field is also found very high with field applied along the  $c$  axis. A small Hall coefficient is also observed in the metallic phase and exhibits a strong temperature dependence, which suggests that the system is likely a multi-band superconductor with high carrier density.

$\text{Pd}_3\text{P}_2(\text{S}_{1-x}\text{Se}_x)_8$  ( $x=0, 0.25$ ) single crystals were grown by the chemical vapor transport (CVD) method<sup>14,15</sup>. As

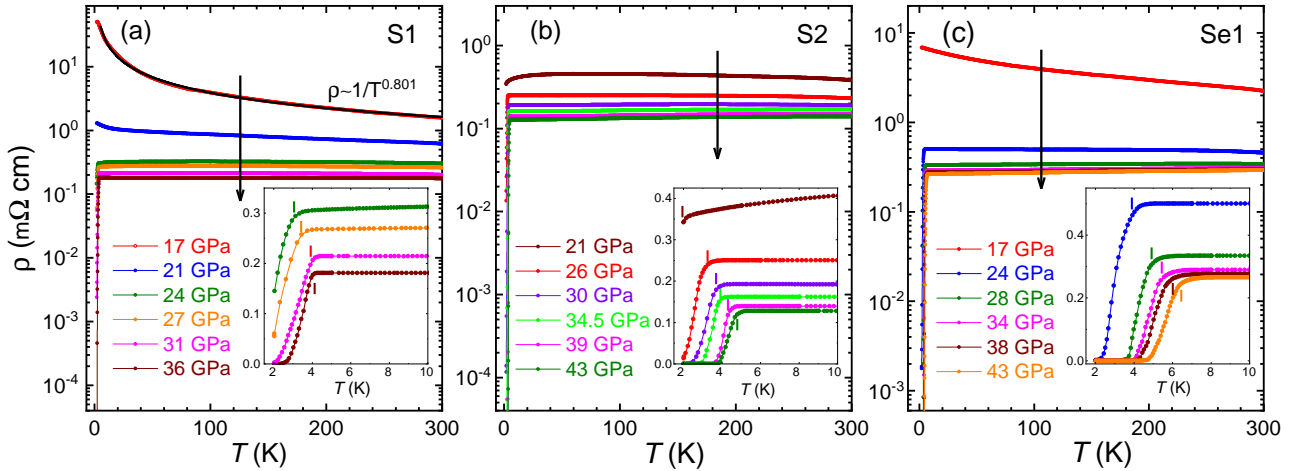


FIG. 2. (a) In-plane resistivity as functions of temperatures of undoped sample S1, measured under different pressures. The black solid line represents a power-law function fit,  $\rho \sim 1/T^{0.801}$ , to the data at 17 GPa. Insert: An enlarged view of low-temperature resistivity. (b)-(c) In-plane resistivity of undoped sample S2 and the Se-doped sample Se1, respectively, and an enlarged view of low-temperature resistivity in the inset. Shot vertical lines in the inset of (a)-(c) mark the emergence of sharp downturn in resistivity, which signals the onset of superconductivity.

shown in Fig. 1(a),  $\text{Pd}_3\text{P}_2\text{S}_8$  has a layered structure with S1-Pd-S1-P-S2 stacked sequentially along the  $c$  axis, and Pd atoms form a perfect kagome structure. Se doping replaces S atoms randomly and enhances the interlayer coupling<sup>15</sup>, which leads to a larger dispersion and a reduction of gap of the flat band. Note that  $x=0.25$  is the maximal Se doping level currently available<sup>15</sup>.

We performed high-pressure transport measurements with a BeCu diamond anvil cell (DAC). Diamond anvils of 300  $\mu\text{m}$  culets and a Rhenium gasket covered with cubic boron nitride (cBN) powder were used, with no pressure transmitting medium filled in. The highest achievable pressure we achieved is 43 GPa. The pressures were calibrated by the Raman spectrum from the culet of a top diamond anvil and fluorescence from the ruby using a Raman microscope (WITec Alpha 300R). For the transport measurements, the DAC, with sample loaded inside, is cooled in a Quantum Design Physical Property Measurement System (PPMS-14T). The in-plane resistivity and the Hall resistivity of samples were performed by the standard van der Pauw method. Three single crystals, cut into a dimensions of  $100 \times 100 \times 20 \mu\text{m}^3$ , were measured. Two of them are undoped, labeled as S1 and S2 respectively, and one is doped, labeled as Se1.

The resistivity of three crystals is first measured with increasing pressures at zero field, and cooled from 300 K down to 2 K. Detailed data are shown as functions of temperatures in Fig. 2(a)-(c). At ambient pressure, the resistance  $\rho$  of all three samples is large at room temperature and is barely measurable at low temperatures. This is consistent with the gapped behavior, where all the bands are away from the Fermi surface<sup>15</sup>. With applied pressure, the resistivity  $\rho$  decreases with pressure for all samples, as shown in Fig. 2(a)-(c). For sample S1, the insulating behavior still holds under pressures of 17 and 21 GPa, as shown by the increase of resistivity upon cooling.

At 17 GPa, the conductivity of sample S1 is found to fol-

low a power-law temperature dependence, that is,  $\rho \sim 1/T^\alpha$  with the power-law exponent  $\alpha = 0.801 \pm 0.001$ , as shown by the fit in Fig. 2(a). The fitting holds in nearly two orders of temperature range below 300 K. By contrast, our data cannot be well fit to a gap function. This power-law temperature dependence of conductivity suggests that insulating behavior is caused by strong electron localization, as a result of disorder in the system<sup>37,38</sup>. In fact, it is found that  $\alpha = 1$  for two-dimensional (2D) systems<sup>39</sup> and  $\alpha$  ranges between 1/3 and 1/2 for 3D systems<sup>38,40</sup>. Our value of  $\alpha \approx 0.8$  suggests that the system crossovers from the 2D to 3D at 17 GPa, which suggests that interlayer coupling is strong enhanced under pressure. Note that the sample at the ambient pressure shows a high quality as revealed by our XRD data<sup>15</sup>, which leads us to speculate that the disorder effect is either an intrinsic pressure-induced structural disorder of the material, or brought in by pressure inhomogeneity under such high pressures.

A very weak upturn in resistivity is still observed at 21 GPa for sample S1, which suggests that the insulating behavior tends to be suppressed at pressures above 20 GPa. At and above 23 GPa, the resistivity decreases weakly upon cooling, which is a clear signature of a metallic behavior. An enlarged view of the low-temperature resistivity, at pressures above 20 GPa, are further demonstrated in the inset of Fig. 2(a). A high conductivity is seen with resistivity less than 0.5  $\text{m}\Omega \text{ cm}$  at room temperature. Since the resistivity does not show a large upturn upon cooling at low temperatures, a metallic, rather than an insulating behavior, is clearly established with pressure above 20 GPa.

Therefore, an insulating to metallic transition is revealed at about 20 GPa in sample S1. Similar transition is also observed for sample S2 and Se2, as shown in Fig. 2(b)-(c). Interestingly, the insulating to metallic transition for all three samples occurs at pressures close to 20 GPa, as shown by the disappearance of the resistivity upturn in Fig. 2(b)-(c). High-pressure XRD measurements are requested to verify if

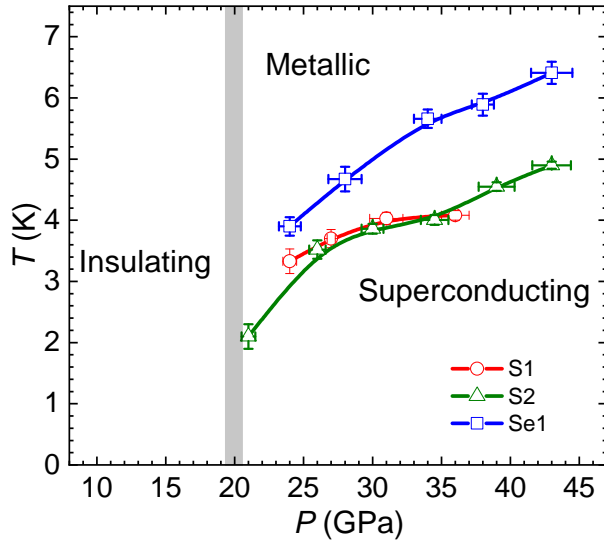


FIG. 3. The high-pressure phase diagram established on sample S1, S2, and Se1. The insulating (metallic) phase labels the regime where a prominent resistivity upturn is observed (absent) upon cooling. Open circles, triangles, and squares represent the onset  $T_C$  of three samples, with the superconducting phase located below.

the change of the conducting behavior is accompanied with a structural transition.

When the metallic behavior is established at high temperatures, a sudden drop of resistivity for all three samples is observed when further cooled, as shown in the inset of Fig. 2(a)-(c). At even lower temperatures, zero resistivity is reached, which is clear evidence of superconductivity. The superconducting transition temperature, labeled as  $T_C$ , is marked by the onset temperature of sharp downturns in resistivity, as shown in the inset of Fig. 2(a)-(c). It is noticed that  $T_C$  rises continuously with pressure up to 43 GPa.

The  $T_C$  is then determined and plotted as functions of pressures for three samples in the phase diagram in Fig. 3. Below 20 GPa, an insulating phase is established by the prominent resistivity upturn; whereas above 20 GPa, the absence of resistivity upturn reveals an onset of a metallic phase which turns into a superconductor at low temperatures. The superconducting transition temperature  $T_C$  rises monotonically with pressure for both the undoped and the doped crystals. For the measured pressure range, the  $T_C$  increases nearly linearly with pressure, at least up to 43 GPa. The slope is determined as  $dT_C/dP = 0.13 \pm 0.03$  K/GPa for all samples. At pressures above 30 GPa, a small increase in  $dT_C/dT$  is also observed, which suggests that a higher  $T_C$  should be achieved at high pressures above 43 GPa.

It is also interesting to note that the  $T_C$  for the Se-doped one is about 1.5 K higher than the undoped one in the whole pressure range. This level of Se doping is equivalent to an applied pressure of 12 GPa comparing the value  $dT_C/dP$ , which suggests that Se doping acts as a chemical pressure, consistent with the LDA calculations that Se doping enhances interlayer coupling<sup>15</sup>. However, superconductivity is not observed in the Se-doped compounds with pressure below 20 GPa, which sug-

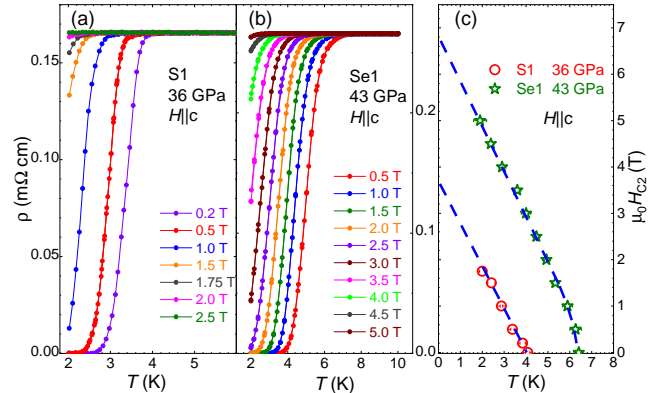


FIG. 4. (a)-(b) Resistivity of sample S1 and Se1, as functions of temperatures measured with fields applied along the  $c$  axis, under pressure of 36 GPa and 43 GPa, respectively. (c) The out-of-plane  $H_{C2}$  of sample S1 and Se1 as functions of temperatures.

gests that disorder, induced by external-pressure as revealed by the power-law temperature dependence of resistivity at low pressures, is highly effective to prohibit superconductivity for both the undoped and the doped compounds.

The out-of-plane upper critical field of superconductivity is also studied by the resistivity measurements with field applied along the crystalline  $c$  axis. The resistivity of sample S1 and Se1 are shown as functions of temperatures in Fig. 4(a)-(b) with different fields, each under a fixed pressure. For each fixed field, the resistivity of sample S1 measured at 36 GPa, as shown in Fig. 4(a), first rises from zero with increasing temperature. Above a specific temperature, resistivity exhibits a level off, which signals the disappearance of superconductivity; then the field is defined as the upper critical field  $H_{C2}$  at that temperature. The  $H_{C2}$  of sample Se1 is also determined in the same way with data shown in Fig. 4(b), under a fixed pressure of 43 GPa.

The  $H_{C2}$  of both crystals is plotted as functions of temperatures in Fig. 4(c), which decreases with temperature. At low temperatures,  $H_{C2}$  drops almost linearly with field. Extrapolation to the zero temperature limit gives  $H_{C2}(T=0) \approx 3.7$  T for sample S1, and  $H_{C2}(0) \approx 6.8$  T for sample Se1. Considering the onset  $T_C$  at zero field is about 4 K (6.4 K) for Sample S1 (Se1), the zero temperature  $H_{C2}$  is then about 50% of the Pauli limit<sup>41-43</sup>, assuming  $g=2$ . Such a high out-of-plane  $H_{C2}$  suggests that the system is likely a 3D superconductor, which is consistent with the resistivity measurements where a 2D to 3D crossover is already observed at 17 GPa as discussed above. Note that a high out-of-plane critical field is also reported in the iron-based superconductors<sup>44</sup>.

To further understand the carrier properties, the Hall resistivity  $\rho_{xy}$  on sample S1 is measured with field applied along the  $c$  axis, under a pressure of 36 GPa. As shown in Fig. 5(a),  $\rho_{xy}$ , plotted as functions of fields measured at different temperatures, shows a linear field dependence with field up to 4 T. By taking the slope of the Hall resistivity, the Hall coefficient  $R_H$  is then calculated and plotted as a function of temperatures in Fig. 5(b).  $R_H$  stays positive with temperature from 200 K to 8K, which suggests that the major carriers are the

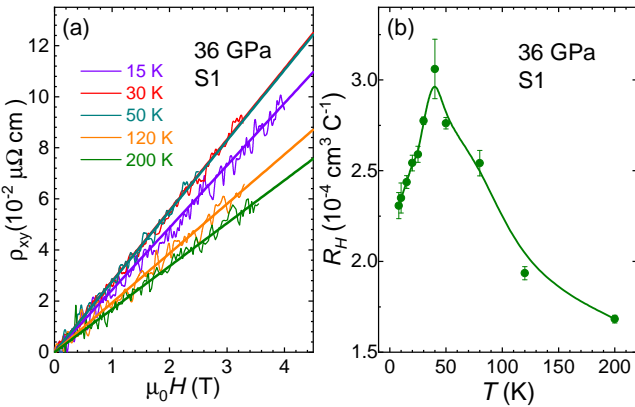


FIG. 5. (a) The in-plane Hall resistivity  $\rho_{xy}$  of sample S1 as functions of fields applied along the  $c$  axis, measured at different temperatures under a constant pressure 36 GPa. The straight lines are linear functional fits to the data to calculate the Hall coefficient  $R_H$ . (b) The obtained  $R_H$  as a function of temperature.

hole type in the system under pressure. However,  $R_H$  changes largely with temperature and is peaked at about 40 K. Such a dramatic temperature dependent suggests that the compounds either have multi electronic bands on the Fermi surface<sup>45,46</sup>, and/or have strong electron correlations<sup>46,47</sup>.

In fact, the values of  $R_H$  in the whole temperature range is very small, whose peaked value reads  $3 \times 10^{-4} \text{ cm}^3 \text{C}^{-1}$  at 40 K. Taking the value of  $R_H$  at 8 K, the carrier concentration is estimated as  $2.70 \times 10^{22} \text{ cm}^{-3}$  at this pressure, assuming a single band. However, this would suggests that each unit cell contains an excessive carrier density of 9.31 holes per unit cell, which is unlikely. On the other hand, if the system contains both hole and electron types of carriers, the value of  $R_H$  can be very small as observed. Together with the large temperature-dependent  $R_H$  as described above, a pressure induced multi-band system, with both electron and hole types of carriers on the Fermi surface, is strongly suggested for the high pressure phase.

As for the hole band, we think that the  $d_{z^2}$  band of  $\text{Pd}^{2+}$  may play an essential role, as it is only slightly below the

Fermi surface, with a weak but finite dispersion already observed in the Se-doped compounds at the ambient pressure<sup>15</sup>. With applied pressure, the enhanced interlayer coupling would induce stronger dispersion on this band and make it closer to the Fermi surface. Furthermore, LDA calculations suggest that a  $d_{x^2-y^2}$  orbital is located at about 1.5 eV above the Fermi surface<sup>15</sup>, which may become the electron band at high pressures. Future LDA calculations under pressure are requested for verification.

To our knowledge, this is the first superconductor derived from a Kagome compound with a flat band. However, we cannot make conclusions on the flat band and its relation with superconductivity by the current data. Future studies with the high-pressure XRD and LDA calculation are requested to address the band structure, the correlation effect, and the nature of superconductivity of the high pressure phase.

In summary, our high-pressure transport studies on the undoped and the Se-doped  $\text{Pd}_3\text{P}_2\text{S}_8$  reveal that the resistivity changes from an insulating to an metallic behavior at about 20 GPa. The power-law temperature dependence of conductivity at low pressure suggests a high level of disorder induced by pressure, with a 2D to 3D crossover. Superconductivity is observed in the metallic phase for all the compounds. The out-of-plane  $H_{C2}$  is high, which again suggests a 3D nature of the system. The superconducting transition temperature  $T_C$  rises with pressure at least up to 43 GPa. Se doping by 25% further enhances  $T_C$  by 1.5 K, which is consistent with a chemical pressure effect. Our data suggests that the high-pressure phase is likely a multi-band system with both electron and hole bands on the Fermi surface, as revealed by the small value of the Hall coefficient and its large temperature dependence.

This work is supported by the National Natural Science Foundation of China under Grants No. 51872328 and 12134020, the Ministry of Science and Technology of China under Grants No. 2016YFA0300504, the China Postdoctoral Science Foundation under Grant No. 2020M680797, the Fundamental Research Funds for the Central Universities and the Research Funds of Renmin University of China under Grants No. 21XNLG18 and No. 18XNLG24.

\* These authors contributed equally to this study.

† hlei@ruc.edu.cn

‡ yuan@qdu.edu.cn

§ zhangjs@ncepu.edu.cn

¶ wqyu-phy@ruc.edu.cn

<sup>1</sup> P.W. Anderson, Science **235**, 1196 (1987).

<sup>2</sup> W.H. Ko, P.A. Lee, and X.G. Wen, Phys. Rev. B **79**, 214502 (2009).

<sup>3</sup> T.H. Han, J.S. Helton, S.Y. Chu, D.G. Nocera, J.A. Rodriguez-Rivera, C. Broholm, and Y.S. Lee, “Fractionalized excitations in the spin-liquid state of a kagome-lattice antiferromagnet,” Nature **492**, 406 (2012).

<sup>4</sup> J.S. Wen, S.L. Yu, S.Y. Li, W.Q. Yu, and J.X. Li, npj Quantum Mater. **4**, 12 (2019).

<sup>5</sup> Y. Wei, X.Y. Ma, Z.L. Feng, Y.C. Zhang, L. Zhang, H.X. Yang,

Y. Qi, Z.Y. Meng, Y.C. Wang, Y.G. Shi, and S.L. Li, Chin. Phys. Lett. **38**, 097501 (2021).

<sup>6</sup> Z.Y. Lin, J.H. Choi, Q. Zhang, W. Qin, S. Yi, P.D. Wang, L. Li, Y.F. Wang, H. Zhang, Z. Sun, L.M. Wei, S.B. Zhang, T.F. Guo, Q.Y. Lu, J.H. Cho, C.G. Zeng, and Z.Y. Zhang, Phys. Rev. Lett. **121**, 096401 (2018).

<sup>7</sup> J.X. Yin, S.T. Zhang, G.Q. Chang, Q. Wang, S.S. Tsirkin, Z. Guguchia, B. Lian, H.B. Zhou, K. Jiang, I. Belopolski, N. Shumiya, D. Multer, M. Litskevich, T.A. Cochran, H. Lin, Z.Q. Wang, T. Neupert, S. Jia, H.C. Lei, and M.Z. Hasan, Nat. Phys. **15**, 443 (2019).

<sup>8</sup> M.G. Kang, L.D. Ye, S.A. Fang, J.S. You, A. Levitan, M.Y. Han, J.I. Facio, C. Jozwiak, A. Bostwick, E. Rotenberg, M.K. Chan, R.D. McDonald, D. Graf, K. Kaznatcheev, E. Vescovo, D.C. Bell, E. Kaxiras, J. van den Brink, M. Richter, M. Prasad Ghimire, J.G.

- Checkelsky, and R. Comin, *Nat. Mater.* **19**, 163 (2020).
- <sup>9</sup> M.G. Kang, S.A. Fang, L.D. Ye, H.C. Po, J. Denlinger, C. Jozwiak, Bostwick A., E. Rotenberg, E. Kaxiras, J.G. Checkelsky, and R. Comin, *Nat. Commun.* **11**, 4004 (2020).
- <sup>10</sup> Z.H. Liu, M. Li, Q. Wang, G.W. Wang, C.H.P. Wen, K. Jiang, X.L. Lu, S.C. Yan, Y.B. Huang, D.W. Shen, J.X. Yin, Z.Q. Wang, Z.P. Yin, H.C. Lei, and S.C. Wang, *Nat. Commun.* **11**, 4002 (2020).
- <sup>11</sup> M. Li, Q. Wang, G.W. Wang, Z.H. Yuan, W.H. Song, R. Lou, Z.T. Liu, Y.B. Huang, Z.H. Liu, H.C. Lei, Z.P. Yin, and S.C. Wang, *Nat. Commun.* **12**, 3129 (2021).
- <sup>12</sup> M.Y. Han, H. Inoue, S.A. Fang, C. John, L.D. Ye, M.K. Chan, D. Graf, T. Suzuki, M.P. Ghimire, W.J. Cho, E. Kaxiras, and J.G. Checkelsky, *Nat. Commun.* **12**, 5345 (2021).
- <sup>13</sup> L.D. Ye, S.A. Fang, M.G. Kang, J. Kaufmann, Y.H. Lee, J. Denlinger, C. Jozwiak, A. Bostwick, E. Rotenberg, E. Kaxiras, D.C. Bell, O. Janson, R. Comin, and J.G. Checkelsky, (2021), [arXiv:2106.10824](https://arxiv.org/abs/2106.10824).
- <sup>14</sup> S. Park, S. Kang, H. Kim, K.H. Lee, P. Kim, S. Sim, N. Lee, B. Karuppannan, J. Kim, J. Kim, K.I. Sim, M.J. Coak, Y. Noda, C.H. Park, J.H. Kim, and J.G. Park, *Sci. Rep.* **10**, 20998 (2020).
- <sup>15</sup> S.H. Yan, B.C. Gong, L. Wang, J.Z. Wu, Q.W. Yin, X.Y. Cao, X. Zhang, X.F. Liu, Z.Y. Lu, K. Liu, and H.C. Lei, (2021), [arXiv:2111.11222](https://arxiv.org/abs/2111.11222).
- <sup>16</sup> E.K. Liu, Y. Sun, N. Kumar, L. Muechler, A.I. Sun, L. Jiao, S.Y. Yang, D.F. Liu, A.J. Liang, Q.N. Xu, J. Kroder, V. Süß, H. Borrman, C. Shekhar, Z.S. Wang, C.Y. Xi, W.H. Wang, W. Schnelle, S. Wirth, Y.L. Chen, Sebastian T. B. Goennenwein, and C. Felser, *Nat. Phys.* **14**, 1125 (2018).
- <sup>17</sup> L.D. Ye, M.G. Kang, J.W. Liu, F. Von Cube, C.R. Wicker, T. Suzuki, C. Jozwiak, A. Bostwick, E. Rotenberg, D.C. Bell, L. Fu, R. Comin, and J.G. Checkelsky, *Nature* **555**, 638 (2018).
- <sup>18</sup> Q.W. Yin, Z.J. Tu, C.S. Gong, Y. Fu, S.H. Yan, and H.C. Lei, *Chin. Phys. Lett.* **38**, 037403 (2021).
- <sup>19</sup> K.Y. Chen, N.N. Wang, Q.W. Yin, Y.H. Gu, K. Jiang, Z.J. Tu, C.S. Gong, Y. Uwatoko, J.P. Sun, H.C. Lei, J.P. Hu, and J.G. Cheng, *Phys. Rev. Lett.* **126**, 247001 (2021).
- <sup>20</sup> L.P. Nie, K.L. Sun, W.R. Ma, D.W. Song, L.X. Zheng, Z.W. Liang, P. Wu, F.H. Yu, J. Li, M. Shan, D. Zhao, S.J. Li, B.L. Kang, Z.M. Wu, Y.B. Zhou, K. Liu, Z.J. Xiang, J.J. Ying, Z.Y. Wang, T. Wu, and X.H. Chen, *Nature* (2022).
- <sup>21</sup> X.L. Feng, K. Jiang, Z.Q. Wang, and J.P. Hu, *Sci. Bull.* **66**, 1384 (2021).
- <sup>22</sup> S.L. Ni, S. Ma, Y.H. Zhang, J. Yuan, H.T. Yang, Z.Y.W. Lu, N.N. Wang, J.P. Sun, Z. Zhao, D. Li, S.B. Liu, H. Zhang, H. Chen, K. Jin, J.G. Cheng, L. Yu, F. Zhou, X.L. Dong, J.P. Hu, H.J. Gao, and Z.X. Zhao, *Chin. Phys. Lett.* **38**, 057403 (2021).
- <sup>23</sup> A. Mielke, *J. Phys. A: Math. Gen.* **25**, 4335 (1992).
- <sup>24</sup> M.L. Kiesel, C. Platt, and R. Thomale, *Phys. Rev. Lett.* **110**, 126405 (2013).
- <sup>25</sup> M. Imada and M. Kohno, *Phys. Rev. Lett.* **84**, 143 (2000).
- <sup>26</sup> S. Miyahara, S. Kusuta, and N. Furukawa, *Physica C: Superconductivity* **460**, 1145 (2007).
- <sup>27</sup> E. Tang, J.W. Mei, and X.G. Wen, *Phys. Rev. Lett.* **106**, 236802 (2011).
- <sup>28</sup> A. Mielke, *J. Phys. A: Math. Gen.* **24**, 3311 (1991).
- <sup>29</sup> H. Tasaki, *Rep. Prog. Phys.* **99**, 489 (1998).
- <sup>30</sup> Y. Cao, V. Fatemi, A. Demir, S.A. Fang, S.L. Tomarken, J.Y. Luo, J.D. Sanchez-Yamagishi, K. Watanabe, T. Taniguchi, E. Kaxiras, R.C. Ashoori, and P. Jarillo-Herrero, *Nature* **556**, 80 (2018).
- <sup>31</sup> Y. Cao, V. Fatemi, S.A. Fang, K. Watanabe, T. Taniguchi, E. Kaxiras, and P. Jarillo-Herrero, *Nature* **556**, 43 (2018).
- <sup>32</sup> Z. Li, J. Zhuang, L. Wang, H. Feng, Q. Gao, X. Xu, W. Hao, X. Wang, C. Zhang, K. Wu, S.X. Dou, L. Chen, Z. Hu, and Y. Du, *Sci. Adv.* **4**, eaau4511 (2018).
- <sup>33</sup> L. Wang, E.M. Shih, A. Ghiotto, L.D. Xian, D.A. Rhodes, C. Tan, M. Claassen, D.M. Kennes, Y.S. Bai, B.H. Kim, K. Watanabe, T. Taniguchi, X.Y. Zhu, J. Hone, A. Rubio, A.N. Pasupathy, and C.R. Dean, *Nat. Mater.* **19**, 861 (2020).
- <sup>34</sup> H. Zi, L.X. Zhao, X.Y. Hou, L. Shan, Z.A. Ren, G.F. Chen, and C. Ren, *Chin. Phys. Lett.* **37**, 097403 (2020).
- <sup>35</sup> X. Chen, X.H. Zhan, X.J. Wang, J. Deng, X.B. Liu, X. Chen, J.G. Guo, and X.L. Chen, *Chin. Phys. Lett.* **38**, 057402 (2021).
- <sup>36</sup> W.R. Meier, M.H. Du, S. Okamoto, N. Mohanta, A.F. May, M.A. McGuire, C.A. Bridges, G.D. Samolyuk, and B.C. Sales, *Phys. Rev. B* **102**, 075148 (2020).
- <sup>37</sup> D.J. Thouless, *Phys. Rev. Lett.* **39**, 1167 (1977).
- <sup>38</sup> D.N. Tsigankov and A.L. Efros, *Phys. Rev. Lett.* **88**, 176602 (2002).
- <sup>39</sup> Z. Ovadyahu and Y. Imry, *J. Phys. Chem. C* **18**, L19 (1985).
- <sup>40</sup> R. Rosenbaum, A. Heines, M. Karpovski, M. Pilosof, and M. Witcomb, *J. Phys. Condens. Matter* **9**, 5413 (1997).
- <sup>41</sup> A. Perez-Gonzalez, *Phys. Rev. B* **54**, 16053 (1996).
- <sup>42</sup> P. Fulde, *Adv. Phys.* **22**, 667 (1973).
- <sup>43</sup> D. Nakamura, T. Adachi, K. Omori, Y. Koike, and S. Takeyama, *Sci. Rep.* **9**, 16949 (2019).
- <sup>44</sup> H.Q. Yuan, J. Singleton, F.F. Balakirev, S.A. Baily, G.F. Chen, J.L. Luo, and N.L. Wang, *Nature* **457**, 565 (2009).
- <sup>45</sup> N.W. Ashcroft and N.D. Mermin, *Solid State Physics* (Saunders College Publishing, Philadelphia, 1976) p. 240.
- <sup>46</sup> P.C. Li, F.F. Balakirev, and R.L. Greene, *Phys. Rev. Lett.* **99**, 047003 (2007).
- <sup>47</sup> H.Y. Hwang, B. Batlogg, H. Takagi, H.L. Kao, J. Kwo, R.J. Cava, J.J. Krajewski, and W.F. Peck, *Phys. Rev. Lett.* **72**, 2636 (1994).